International Journal of Numerical Methods for Heat & F...

Boundary layer flow and heat transfer of a non-Newtonian nanofluid over a non-linearly stretching sheet

Macha Madhu Naikoti Kishan A. Chamkha

Boundary layer flow and heat transfer of a non-Newtonian nanofluid over a non-linearly stretching sheet

Received 16 February 2015
Revised 5 May 2015
12 May 2015
18 June 2015
Accepted 18 June 2015

Macha Madhu and Naikoti Kishan
Department of Mathematics, Osmania University, Hyderabad, India, and
A. Chamkha
Department of Mechanical Engineering,
Prince Mohammad Bin Fahd University, Al-Khobar, Saudi Arabia and
Prince Sultan Endowment for Energy and Environment,
Prince Mohammad Bin Fahd University, Al-Khobar, Saudi Arabia

Abstract

Purpose – The purpose of this paper is to study the boundary layer flow and heat transfer of a power-law non-Newtonian nanofluid over a non-linearly stretching sheet.
Design/methodology/approach – The governing equations describing the problem are transformed into a nonlinear ordinary differential equations by suitable similarity transformations. The resulting equations for this investigation are solved numerically by using the variational finite element method.
Findings – It was found that the local Nusselt number increases by increasing the Prandtl number, stretching sheet parameter and decreases by increasing the power-law index, thermophoresis parameter and Lewis number. Increases in the stretching sheet parameter, Prandtl number and thermophoresis parameter decrease the local Sherwood number values. The effects of Brownian motion and Lewis number lead to increases in the local Sherwood number values.
Originality/value – The work is relatively original as very little work has been reported on non-Newtonian nanofluids.
Keywords Heat transfer, Non-Newtonian nanofluid, Boundary layer flow,
Non-linear stretching sheet
Paper type Research paper

Nomenclature

C	nanoparticle volume fraction
C_{f_x}	skin-friction coefficient
D_B	Brownian diffusion
D_T	thermophoretic diffusion coefficient
f	dimensionless stream function
Le	Lewis number
m	velocity exponent parameter
n	power-law fluid index
Nb	Brownian motion parameter
Nt	thermophoresis parameter
Nu_x	Nusselt number
Pr	Prandtl number
r	temperature exponent parameter
Re_x	local Reynolds number
Sh_x	Sherwood number
T	fluid temperature
u,v	velocity components
x,y	Cartesian coordinates

Greek symbols

α_m	thermal diffusivity
ν	kinematic viscosity of the fluid
θ	dimensionless temperature
ϕ	dimensionless nanoparticle volume fraction

International Journal of Numerical Methods for Heat & Fluid Flow
Vol. 26 No. 7, 2016
pp. 2198-2217

0961-5539
DOI 10.1108/HFF-02-2015-0066

ψ stream function
η similarity independent variable

Subscripts
w conditions at the wall
∞ ambient condition

Superscripts
$'$ prime denotes the derivative with respect to η

1. Introduction

Many modern materials and industrial fluids such as particulate slurries (China clay, coal in water, sewage sludge, etc.), multi-phase mixtures (oil-water emulsions, gas-liquid dispersions, froths and foams, butter), pharmaceutical formulations, cosmetics and toiletries, paints, synthetic lubricants, biological fluids (blood, synovial fluid, salvia) and foodstuffs (jams, jellies, soups, marmalades) in their flow characteristics can be sorted into the non-Newtonian fluids. For a non-Newtonian fluid, the viscous stress is a non-linear function of the rate of deformation and the relationship for the power-law fluids given by:

$$\tau_{xy} = \mu \left| \frac{\partial u}{\partial y} \right|^{n-1} \frac{\partial u}{\partial y}$$

where τ_{xy} is the shear stress, μ is the consistency index and n is the power-law index. The fluid is described for $n < 1$ as pseudo-plastic, $n > 1$ as dilatant and $n = 1$ as the Newtonian fluid. Schowalter (1960) was the first to formulate the boundary layer flow of a non-Newtonian fluid and established the conditions for the existence of a similarity solution. A similarity solution to the boundary layer equations for a power-law fluid flowing along a flat plate at 0 degree of angle was obtained by Acrivos *et al.* (1960). The power-law model is widely used to study the pseudo-plastic and dilatant nature of non-Newtonian fluids. Acrivos (1960) was the first to study free convection boundary layer flow of a non-Newtonian power-law fluid along a vertical flat plate for large modified Prandtl numbers. The flow of a power-law fluid over a continuous moving flat plate with constant surface velocity and temperature has been considered by Fox *et al.* (1969). Exact solutions of the equations of motion of non-Newtonian power-law fluids are difficult. The difficulty arises not only due to the non-linearity but also due to the order of the governing differential equations.

The study of flow and heat transfer over a stretching surface issuing from a slit has gained a considerable attention of many researchers due to its importance in many industrial applications. For example, in extrusion of a polymer sheet from a die, the sheet is sometimes stretched. During this process, the properties of the final product depend on the rate of cooling and the stretching rate by drawing such a sheet into a cooling system. Since the pioneering work of Sakiadis (1961) who investigated the boundary layer flow of a viscous fluid past a moving solid surface, various aspects of the problem have been explored by many authors in the past decades. Crane (1970) studied the boundary layer flow of an incompressible viscous fluid toward a linear stretching sheet. Cortell (2007) studied viscous flow and heat transfer over a non-linearly stretching sheet. Andersson and Kumaran (2006) studied the boundary layer flow of a non-Newtonian power-law fluid over a non-linear stretching sheet. Chamkha and Al-Humoud (2007) studied mixed convection heat and transfer of non-Newtonian fluids from a permeable surface embedded in a porous Medium. Kishan and Shashidhar Reddy (2013) and Kishan and Kavitha (2014) studied MHD flow and heat transfer of a non-Newtonian power-law fluid over a stretching surface with viscous dissipation. Mahmoud (2010) investigated the effects of chemical reaction and variable viscosity on the boundary layer flow and heat transfer of a non-Newtonian viscoelastic fluid over a stretching surface immersed in a porous medium.

Keimanesh *et al.* (2011) studied non-Newtonian fluid flow between two parallel plates using the multi-step differential transform method. Rashidi *et al.* (2012) studied non-Newtonian fluid flow and heat transfer over a non-isothermal wedge.

All of the above mentioned investigations are confined only to non-Newtonian fluid over a stretching sheet. However, to the best of the authors' knowledge, the non-Newtonian nanofluid which obeys the power-law model over a non-linear stretching sheet have not been considered. Recent advances in nanotechnology have led to the development of a new innovative class of heat transfer fluids, called nanofluids created by dispersing nanoparticles (10-50 nm) in traditional heat transfer fluids (Choi, 2009). Since, the nanotechnology has been widely used in industrial cooling applications, nuclear reactors, transportation industry (automobiles, trucks and airplanes), micro-electromechanical systems, electronics and instrumentation and biomedical applications (nano-drug delivery, cancer therapeutics and cryopreservation), thus the behavior of non-Newtonian nanofluids could be useful in evaluating the possibility of heat transfer enhancement in various processes in these industries. Therefore, many studies have focussed on nanofluids nowadays. For instance, Khanafer *et al.* (2003) examined heat transfer performance of nanofluids inside an enclosure taking into account the solid particle dispersion. Bachok *et al.* (2010) examined the boundary layer of nanofluids over a moving surface when the plate is assumed to move in the same or opposite directions to the free stream. The boundary layer flow induced in a nanofluid due to a linearly stretching sheet that was investigated by Makinde and Aziz (2011). Kuznetsov and Nield (2010) examined the natural convection flow of nanofluid over a vertical plate. Some relevant work on nanofluids can be seen from the list of references (Choi *et al.*, 2001; Khan and Pop, 2010; Lotfi *et al.*, 2010). Nield (2011) studied the onset of convection in a layer of a porous medium which is filled with non-Newtonian nanofluids of power-law type. Ellahi *et al.* (2012) have elaborated that non-Newtonian nanofluids have potential roles in physiological transport as biological solutions and also in polymer melts, paints, etc. Gorla and Chamkha (2011, 2013) investigated natural convective boundary layer flow over a vertical plate embedded in a porous medium saturated with a non-Newtonian nanofluid. Recently, Chamkha *et al.* (2014) studied non-similar solutions for mixed convection boundary layer flow along a wedge embedded in a porous medium saturated by a non-Newtonian nanofluid.

Kuznetsov and Nield (2014) in their paper employed boundary conditions on the nanoparticle fraction more realistic physically. They assumed that one can control the volume of the nanoparticle fraction at the wall, but rather that the nanoparticles flux at the wall is 0. In the present paper, we have considered the boundary condition of the nanoparticle fraction at the wall given by Kuznetsov and Nield (2014).

To the best of the authors' knowledge, no investigations has been reported regarding the study of non-Newtonian nanofluids obeying the power-law fluid model over a nonlinear stretching sheet. The principal aim of this paper is to study the boundary layer flow and heat transfer of a power-law non-Newtonian nanofluid over a non-linearly stretching sheet. The governing equations are solved numerically by using the variational finite element method.

2. Mathematical formulation

Consider, steady laminar two-dimensional boundary layer flow due to a stretching sheet in a quiescent viscous incompressible nanofluid obeying power-law model (see Metzner, 1965; Hang and Shi-Jun, 2009). The flow is generated as a consequence of non-linear stretching of the boundary sheet, caused by simultaneous application of two equal and opposite forces along x-axis, while keeping the origin fixed in the fluid of the

ambient temperature T_∞. The positive x-coordinate is measured along the direction of the motion, with the slot at the origin. The positive y-coordinate is measured normal to the surface of the sheet and is positive from the sheet to the fluid. The continuous stretching sheet is assumed to have a non-linear velocity and prescribed temperature of the form $U(x) = bx^m$ and $T_w(x) = T_\infty + Ax^r$, respectively, where b is the stretching constant, x is the distance from the slot; A is a constant whose value depends upon the properties of the fluid. Here, m and r are the velocity and temperature exponents, respectively. Under these assumptions, the basic equations governing the flow and heat, mass transfer in usual notation are:

$$\frac{\partial u}{\partial x} + \frac{\partial v}{\partial y} = 0 \tag{1}$$

$$u\frac{\partial u}{\partial x} + v\frac{\partial u}{\partial y} = -\nu\frac{\partial}{\partial y}\left(-\frac{\partial u}{\partial y}\right)^n \tag{2}$$

$$u\frac{\partial T}{\partial x} + v\frac{\partial T}{\partial y} = \alpha\frac{\partial^2 T}{\partial y^2} + \tau\left[D_B\frac{\partial C}{\partial y}\frac{\partial T}{\partial y} + \frac{D_T}{T_\infty}\left(\frac{\partial T}{\partial y}\right)^2\right] \tag{3}$$

$$u\frac{\partial C}{\partial x} + v\frac{\partial C}{\partial y} = D_B\frac{\partial^2 C}{\partial y^2} + \frac{D_T}{T_\infty}\frac{\partial^2 T}{\partial y^2} \tag{4}$$

The relevant boundary conditions of the problem are:

$$u = U, v = 0, T = T_w, D_B\frac{\partial C}{\partial y} + \frac{D_T}{T_\infty}\frac{\partial T}{\partial y} = 0, \quad at \quad y = 0, \tag{5}$$

$$u \to 0, T \to T_\infty, C \to C_\infty \quad as \quad y \to \infty \tag{6}$$

where u and v, are the velocity components along x and y axes, respectively. T is the temperature of the fluid, C is the nanoparticle volume fraction, σ is the electric conductivity, ρ is the fluid density, α_m is the thermal diffusivity, D_B is the Brownian diffusion coefficient and D_T is the thermophoretic diffusion coefficient. The first term in the right hand side of the Equation (2), is the shear rate ($\partial u/\partial y$) has been assumed to be negative throughout the boundary layer since the stream wise velocity component u decreases monotonically with the distance y from the moving surface (for continuous stretching surface). A rigorous derivation and subsequent analysis of the boundary layer equations, for power-law fluids, were recently provided by Denier and Dabrowski (2004). They focussed on boundary layer flow driven by free stream $U(x) \approx x^m$ i.e., of Falkner-Skan type. Such boundary layer flows are driven by a stream wise pressure gradient $-dp/dx = \rho(du/dx)$ set up by the external free stream outside the viscous boundary layer. In the present context no driving pressure gradient is present. Instead the flow is driven solely by the stretching surface, which moves with a prescribed velocity $U(x)$. The boundary condition for nanoparticle volume fraction is taken as given by Kuznetsov and Nield (2014).

In terms of the standard definition of the stream function such that $u = \partial\psi/\partial y$ and $v = -\partial\psi/\partial x$ and introducing the following transformation variables:

$$\psi = Ux(Re_x)^{-\frac{1}{n+1}} f(\eta), \theta = \frac{T - T_\infty}{T_w - T_\infty}, \phi = \frac{C}{C_\infty}, \eta = \frac{y}{x}(Re_x)^{\frac{1}{n+1}} \tag{7}$$

where the local Reynolds number is defined by $Re_x = U^{2-n}x^n/\nu$.

Substituting the dimensionless parameters of Equation (7) into Equations (2)-(4) gives:

$$n(-f'')^{(n-1)}f''' + \left(\frac{2mn-m+1}{n+1}\right)ff'' - mf'^2 = 0 \tag{8}$$

$$\frac{1}{Pr}\theta'' + \left(\frac{2mn-m+1}{n+1}\right)f\theta' - rf'\theta + Nb\theta'\phi' + Nt\theta'^2 = 0 \tag{9}$$

$$\phi'' + \left(\frac{2mn-m+1}{n+1}\right)Lef\phi' + \frac{Nt}{Nb}\theta'' = 0 \tag{10}$$

The boundary conditions are transformed as:

$$f(0) = 0, f'(0) = 1, \theta(0) = 1, Nb\phi'(0) + Nt\theta'(0) = 0,$$
$$f'(\infty) \to 0, \theta(\infty) \to 0, \phi(\infty) \to 0, \tag{11}$$

The non-dimensional parameters appearing in Equations (11)-(13) are as follows:

$$Pr = \frac{Ux}{\alpha}(Re_x)^{\frac{-2}{n+1}}, Nb = \frac{\tau D_B(C_w - C_\infty)}{Ux}(Re_x)^{\frac{2}{n+1}},$$
$$Nt = \frac{\tau D_T(T_w - T_\infty)}{UxT_\infty}(Re_x)^{\frac{2}{n+1}}, Le = \frac{Ux}{D_B}(Re_x)^{\frac{-2}{n+1}}.$$

The physical quantities of interest are the skin-friction coefficient C_{fx}, the Nusselt number Nu_x and Sherwood number Sh_x, which are defined as:

$$C_{f_x} = \frac{2\tau_w}{\rho U^2}, Nu_x = \frac{-x}{T_w - T_\infty}\left(\frac{\partial T}{\partial y}\right)_{y=0}, Sh_x = \frac{-x}{C_\infty}\left(\frac{\partial C}{\partial y}\right)_{y=0} \tag{12}$$

where $\tau_w = (K|(\partial u)/(\partial y)|^{n-1}((\partial u)/(\partial y)))_{y=0}$

Using the non-dimensional variables (7), we obtain:

$$C_{f_x}(Re_x)^{\frac{2}{n+1}} = 2\left|f''(0)\right|^{n-1}f''(0), Nu_x(Re_x)^{\frac{2}{n+1}} = -\theta'(0), Sh_x(Re_x)^{\frac{2}{n+1}} = -\phi'(0) \tag{13}$$

3. Method of solution

3.1 Finite element method

The finite element method is a powerful technique for solving ordinary or partial differential equations. The steps involved in the finite element analysis are as follows:

- discretization of the domain into elements;
- derivation of element equations;
- assembly of element equations;
- imposition of boundary conditions; and
- solution of assembled equations.

To solve the system of simultaneous nonlinear differential Equations (8)-(10), with the boundary conditions (12), first assume:

$$f' = h \tag{14}$$

then the system of Equations (11)-(13) reduced to:

$$n(-h')^{(n-1)}h'' + \left(\frac{2mn-m+1}{n+1}\right)fh' - mh^2 = 0 \tag{15}$$

$$\frac{1}{Pr}\theta'' + \left(\frac{2mn-m+1}{n+1}\right)f\theta' - rh\theta + Nb\theta'\phi' + Nt\theta'^2 = 0 \tag{16}$$

$$\phi'' + \left(\frac{2mn-m+1}{n+1}\right)Lef\phi' + \frac{Nt}{Nb}\theta'' = 0 \tag{17}$$

and the corresponding boundary conditions are reduced as:

$$f(0) = 0, h(0) = 1, \theta(0) = 1, Nb\phi'(0) + Nt\theta'(0) = 0,$$
$$h(\infty) \to 0, \theta(\infty) \to 0, \phi(\infty) \to 0, \tag{18}$$

For computational purposes, here η at ∞ is takes numerically as η_{max} and chosen large enough, so that the solution shows no further change for η larger than η_{max}. The boundary condition for η_{max} (i.e. $\eta \to \infty$) is fixed as $\eta_{max} = 6$, without any loss of generality. The entire flow domain is divided into 1,000 linear line elements of equal size. The linear Lagrange polynomial is used for the typical element.

3.2 Variational formulation

The variational form of the Equations (14)-(17) over a typical element (η_e, η_{e+1}) is given by:

$$\int_{\eta_e}^{\eta_{e+1}} w_1\{f' - h\}d\eta = 0 \tag{19}$$

$$\int_{\eta_e}^{\eta_{e+1}} w_2\left\{n(-h')^{(n-1)}h'' + \left(\frac{2mn-m+1}{n+1}\right)fh' - mh^2\right\}d\eta = 0 \tag{20}$$

$$\int_{\eta_e}^{\eta_{e+1}} w_3\left\{\frac{1}{Pr}\theta'' + \left(\frac{2mn-m+1}{n+1}\right)f\theta' - rh\theta + Nb\theta'\phi' + Nt\theta'^2\right\}d\eta = 0 \tag{21}$$

$$\int_{\eta_e}^{\eta_{e+1}} w_4\left\{\phi'' + \left(\frac{2mn-m+1}{n+1}\right)Lef\phi' + \frac{Nt}{Nb}\theta''\right\}d\eta = 0 \tag{22}$$

where w_1, w_2, w_3 and w_4 are weight functions corresponding to functions f, g, θ and ϕ, respectively.

3.3 Finite element formulation

The finite element model from Equations (19) to (22) by substituting finite element approximations of the form:

$$f=\sum_{j=1}^{2} f_j\psi_j, h=\sum_{j=1}^{2} h_j\psi_j, \theta=\sum_{j=1}^{2} \theta_j\psi_j, \phi=\sum_{j=1}^{2} \phi_j\psi_j$$

with $w_1=w_2=w_3=w_4=\psi_i$, $(i=1,2)$.

Here the shape functions ψ_i for a typical element (η_e, η_{e+1}) are taken as follow.

Linear element:

$$\psi_1^{(e)}=\frac{\eta_{e+1}-\eta}{\eta_{e+1}-\eta_e}, \psi_2^{(e)}=\frac{\eta-\eta_e}{\eta_{e+1}-\eta_e}, \eta_e\leqslant\eta\leq\eta_{e+1}.$$

The finite element model of the equations are expressed by:

$$\begin{bmatrix} [K^{11}] & [K^{12}] & [K^{13}] & [K^{14}] \\ [K^{21}] & [K^{22}] & [K^{23}] & [K^{24}] \\ [K^{31}] & [K^{32}] & [K^{33}] & [K^{34}] \\ [K^{41}] & [K^{42}] & [K^{43}] & [K^{44}] \end{bmatrix} \begin{bmatrix} \{f\} \\ \{h\} \\ \{\theta\} \\ \{\phi\} \end{bmatrix} = \begin{bmatrix} \{b^1\} \\ \{b^2\} \\ \{b^3\} \\ \{b^4\} \end{bmatrix}$$

where $[K^{mn}]$ and $[b^m]$ $(m=1, 2)$ are defined as:

$$K_{ij}^{11}=\int_{\eta_e}^{\eta_{e+1}} \psi_i\frac{d\psi_j}{d\eta}d\eta, K_{ij}^{12}=-\int_{\eta_e}^{\eta_{e+1}} \psi_i\psi_j d\eta, K_{ij}^{13}=K_{ij}^{14}=K_{ij}^{21}=0$$

$$K_{ij}^{22}=\int_{\eta_e}^{\eta_{e+1}} \left[-n\left(\overline{-h'}\right)^{n-1}\frac{d\psi_i}{d\eta}\frac{d\psi_j}{d\eta}+\left(\frac{2mn-m+1}{n+1}\right)\bar{f}\psi_i\frac{d\psi_j}{d\eta}-m\bar{h}\psi_i\psi_j\right]d\eta,$$

$$K_{ij}^{23}=K_{ij}^{24}=K_{ij}^{31}=K_{ij}^{32}=0,$$

$$K_{ij}^{33}=\int_{\eta_e}^{\eta_{e+1}} \left[-\frac{1}{Pr}\frac{d\psi_i}{d\eta}\frac{d\psi_j}{d\eta}+\left(\frac{2mn-m+1}{n+1}\right)\bar{f}\psi_i\frac{d\psi_j}{d\eta}-r\bar{h}\psi_i\psi_j +Nb\overline{\phi'}\psi_i\frac{d\psi_j}{d\eta}+Nt\overline{\theta'}\psi_i\frac{d\psi_j}{d\eta}\right]d\eta,$$

$$K_{ij}^{34}=K_{ij}^{41}=K_{ij}^{42}=0, K_{ij}^{43}=-\frac{Nt}{Nb}\int_{\eta_e}^{\eta_{e+1}}\frac{d\psi_i}{d\eta}\frac{d\psi_j}{d\eta}d\eta,$$

$$K_{ij}^{44}=\int_{\eta_e}^{\eta_{e+1}} \left[-\frac{d\psi_i}{d\eta}\frac{d\psi_j}{d\eta}+Le\left(\frac{2mn-m+1}{n+1}\right)\bar{f}\psi_i\frac{d\psi_j}{d\eta}\right]d\eta.$$

And:

$$b_i^1=0, \quad b_i^2=-n\left(\overline{-h'}\right)^{n-1}\left(\psi_i\frac{dh}{d\eta}\right)_{\eta_e}^{\eta_{e+1}}, \quad b_i^3=-\frac{1}{Pr}\left(1+\frac{4R_d}{3}\right)\left(\psi_i\frac{d\theta}{d\eta}\right)_{\eta_e}^{\eta_{e+1}},$$

$$b_i^4=-\left(\psi_i\frac{d\phi}{d\eta}\right)_{\eta_e}^{\eta_{e+1}}-\frac{Nt}{Nb}\left(\psi_i\frac{d\theta}{d\eta}\right)_{\eta_e}^{\eta_{e+1}}$$

where:

$$\overline{f} = \sum_{i=1}^{2} \overline{f}_i \psi_i, \overline{h} = \sum_{i=1}^{2} \overline{h}_i \psi_i, \overline{h'} = \sum_{i=1}^{2} \overline{h'_i} \psi_i, \overline{\theta'} = \sum_{i=1}^{2} \overline{\theta'_i} \psi_i, \overline{\phi'} = \sum_{i=1}^{2} \overline{\phi'_i} \psi_i$$

Each element matrix is of the order 8×8. The whole domain is divided into 1,000 linear elements of equal size, the element size is taken as $\Delta\eta = 0.006$. At each node four functions are to be evaluated; hence after assembly of all the elemental equations, we obtain a matrix of the order 4,004×4,004. The obtained system is non-linear, therefore an iterative scheme is utilized in the solution. After imposing the boundary conditions the remaining system contains 3,997 equations, which is solved by the Gauss elimination method while maintaining an accuracy of 10^{-5}. The iterative process is terminated when the following condition is satisfied:

$$\sum_i \left| \Phi_i^{j+1} - \Phi_i^j \right| \leqslant 10^{-5}$$

where Φ stands for either f, h, θ or ϕ and j denotes the iterative step.

4. Result and discussion

The system of non-linear coupled ordinary differential Equations (14)-(17) with boundary conditions (19) are solved numerically by using the variational finite element method. In the present study, the computations have been carried out for various flow parameters such as power-law index n, temperature exponent parameter r, velocity exponent parameter m, Prandtl number Pr, thermophoresis Nt, Brownian motion Nb and Lewis number Le. To assess the accuracy of the present computed results for the skin-friction coefficient $f''(0)$ values are shown in Table I. It is observed that from the table comparison of $f''(0)$ values reveals that there is an excellent agreement of our obtained results with those of published work of Hang and Shi-Jun (2009), Andersson and Kumaran (2006) and Chen (2008).

The grid-independence test is also performed to sustain the five decimal-point accuracy. With the help of this test, we have improved the results using successively smaller step sizes for the calculations. Initially, a coarse mesh of 125 elements having a step size $\Delta\eta = 0.048$ has been chosen. Then, increasing the elements four times, we have a medium mesh of 500 elements having a step size of $\Delta\eta = 0.012$. Finally, we have a fine mesh of 1,000 elements having a step size of $\Delta\eta = 0.006$ and get the five decimal-point accuracy in velocity, temperature and nanoparticle volume fraction values.

The Nusselt number and Sherwood number are important physical quantities of engineering interest. The numerical results for the Nusselt number $-\theta'(0)$ and Sherwood number $-\phi'(0)$ values are shown in Table II for the effect of various flow parameters. From Table II, it can be seen that the values of Nusselt number $-\theta'(0)$

Table I. Comparison of $f''(0)$ for various values of n at $m = 1$ in the absence of heat and mass transfer

n	Present results	Hang and Shi-Jun (2009)	Andersson and Kumaran (2006)	Chen (2008)
0.8	−1.028751	−1.02853	−1.029	−1.02919
1.0	−1.00000	−1.00000	−1.000	−1.00000
1.5	−0.98132	−0.98237	−0.981	−0.98056
2.0	−0.98011	−0.97992	−0.981	−0.98000

n	m	Pr	Nb	Nt	Le	$-\theta'(0)$	$-\phi'(0)$
0.75	0.1	7	0.1	0.1	5	1.60527	−1.60477
1.0						1.56864	−1.56722
1.2						1.55497	−1.55452
0.75	−0.2					1.55236	−1.55195
	0					1.58674	−1.58627
	0.2					1.62445	−1.62392
		6				1.47956	−1.4791
		8				1.72202	−1.72148
		10				1.93515	−1.93455
			0.2			1.60527	−0.802387
			0.3			1.60527	−0.534925
			0.4			1.60527	−0.401193
				0.2		1.5304	−3.05985
				0.3		1.45667	−4.36865
				0.4		1.38468	−5.53701
					10	1.56107	−1.5601
					20	1.50866	−1.50679
					30	1.47688	−1.47413

Table II.
Computations of the Nusselt number and Sherwood number for different values of n, m, Pr, Nt, Nt and Le

decreases with the increase of power-law index n, thermophoresis parameter Nt and Lewis number Le. It is also observed that with the increase of Prandtl number Pr and stretching parameter m the Nusselt number $-\theta'(0)$ values increases. The effect of the stretching parameter m, Prandtl number Pr and thermophoresis parameter Nt is to decrease the Sherwood number $-\phi'(0)$ values whereas the values of $-\phi'(0)$ are increases with the increase of power-law index n, Brownian motion Nb and Lewis number Le.

The effect of the power-law index n on the dimensionless velocity f', dimensionless temperature θ and the nanoparticle volume fraction ϕ are shown in Figure 1(a)-(c), respectively. It is found that the velocity with in the boundary layer increases as n increases, a large velocity predicted for the dilatant fluids ($n > 1$) and smaller velocity for pseudo-plastic fluids ($n < 1$) as when compared to a Newtonian fluid ($n = 1$). It is seen from Figure 1(b) and (c) that the temperature and concentration profiles decreases with the increase of n.

For different values of stretching parameter m, Figure 2(a)-(c) shows the dimensionless velocity, temperature and concentration profiles, respectively. From all these figures it can be seen that the effect of an increasing stretching parameter m is to decreases velocity, temperature and concentration profiles. From the acquired results in Figure 2(a), it is noticed that the effect of increasing the value of the velocity exponent parameter m is to reduce the momentum boundary layer thickness. Physically, $m < 0$ implies that the surface is decelerated from the slot, $m = 0$ implies the continuous momentum of a flat surface and $m > 0$ implies that the surface is accelerated from the extended slit.

In order to understand the effect of thermophoresis parameter Nt, the graphs are plotted for temperature in Figure 3(a) and concentration in Figure 3(b) for pseudo-plastic, Newtonian and dilatant fluids. It is clear from the figures that the temperature profiles increases with the increase in Nt. From the Figure 3(b) it can be seen that the effect of Nt on nanoparticle volume fraction is very meager in the vicinity of the boundary and the effect is higher away from the sheet. The variation of temperature

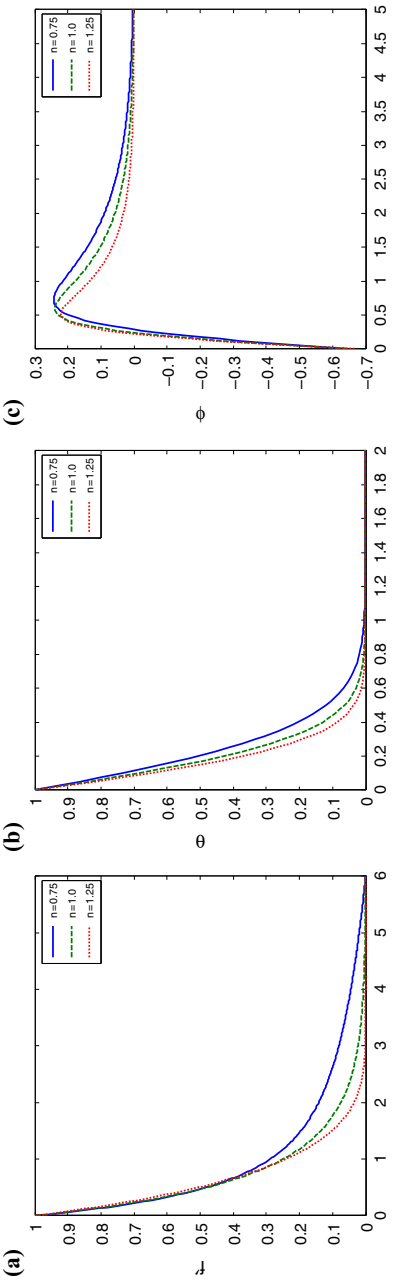

Notes: (a) Velocity; (b) temperature; (c) nanoparticle volume fraction

Figure 1.
Effect of power-law index n on the velocity, temperature and nanoparticle volume fraction profiles

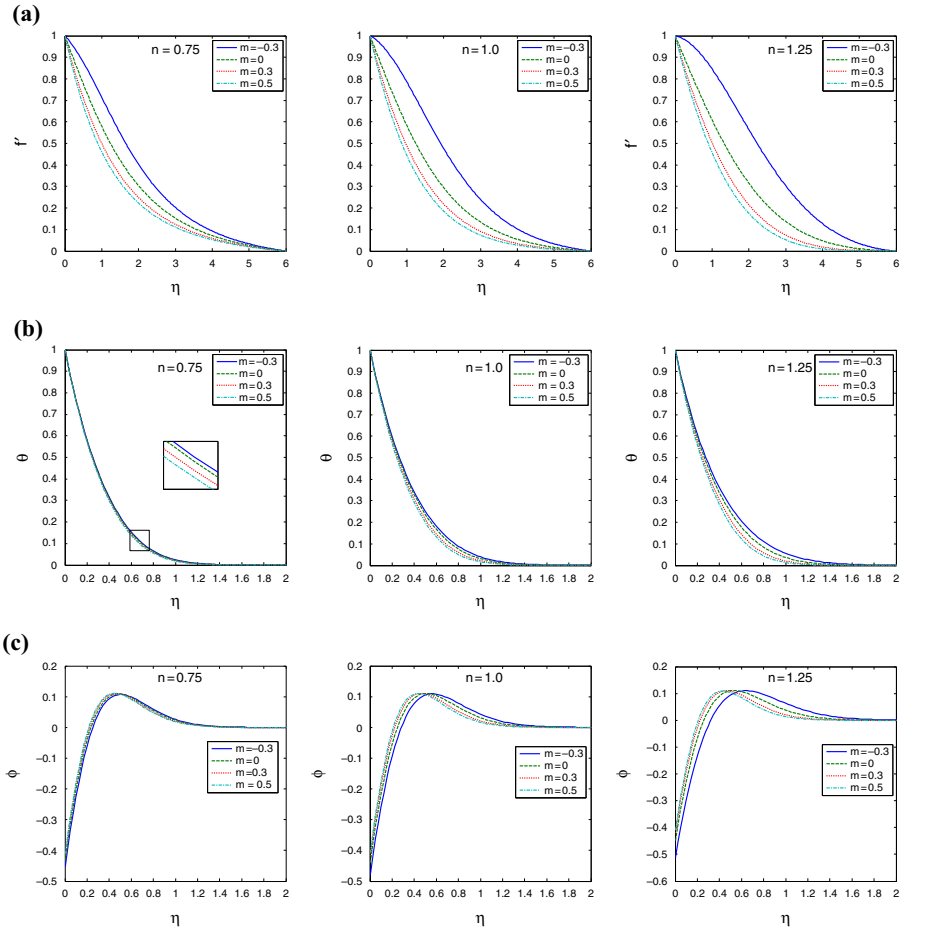

Figure 2.
Effect of m on velocity, temperature and nanoparticle volume fraction profiles for pseudo-plastic, Newtonian and dilatant fluids

Notes: (a) Velocity; (b) temperature; (c) nanoparticle volume fraction

and concentration profiles for pseudo-plastic, Newtonian and dilatant fluids with different values of Brownian motion *Nb* are shown in Figure 4. From this figure it is evident that increasing the values of *Nb* is to decrease the concentration profile.

Figure 5 illustrates temperature profiles for different values of temperature exponent parameter *r* for pseudo-plastic, Newtonian and dilatant fluids, respectively. The effect of increasing values of *r* is to decrease temperature profiles. From the figure it reveals that the effect of *r* is higher in pseudo-plastic ($n < 1$) when compared with the other fluids.

As shown in Figure 6 the non-dimensional temperature profiles decreases as Prandtl number increases for the pseudo-plastic, Newtonian and dilatant fluids. That is an increase in *Pr* means decrease in thermal conductivity and hence there will be a decrease of thermal boundary thickness. The nanoparticles volume fraction profiles is decreased due to the increasing of Lewis number *Le* can be observed from Figure 7. From the definition of Lewis number, a higher value of Lewis number cause

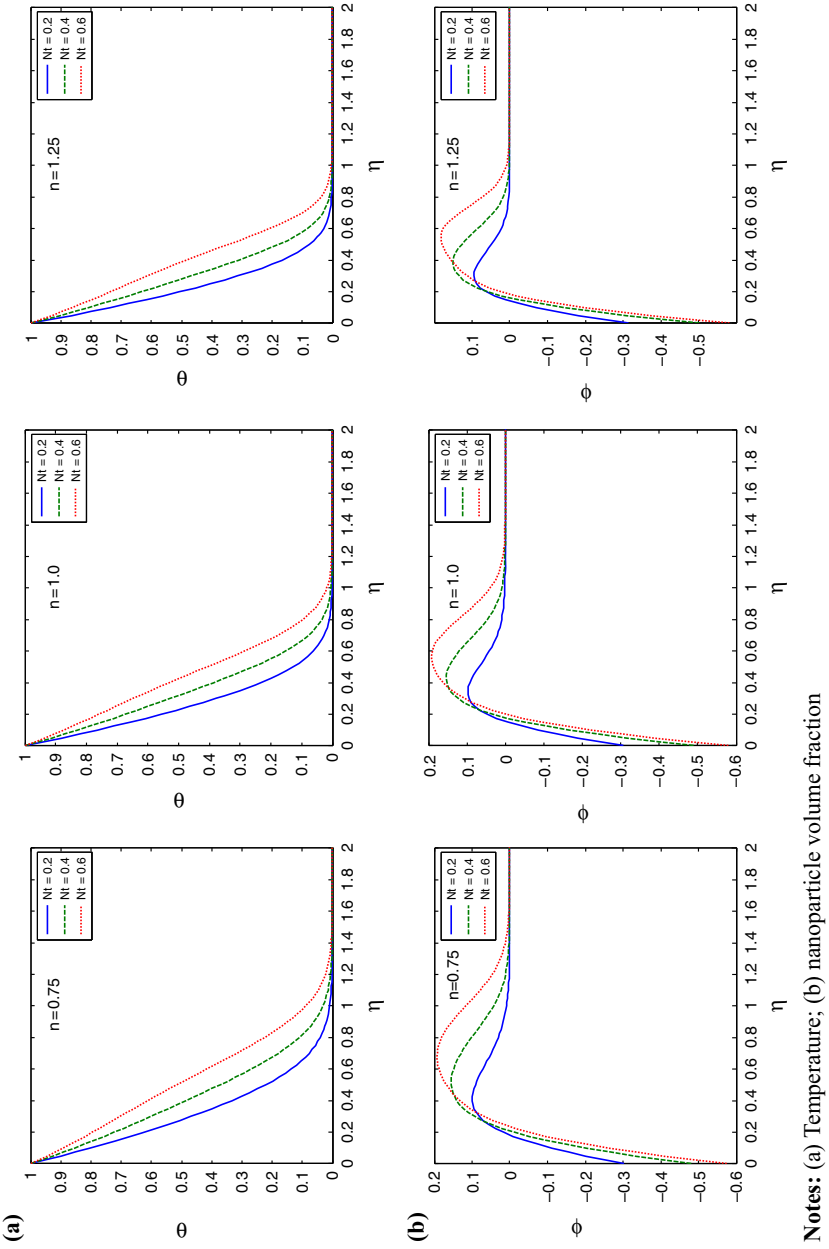

Notes: (a) Temperature; (b) nanoparticle volume fraction

Figure 3.
Effect of Nt on temperature and nanoparticle volume fraction profiles for pseudo-plastic, Newtonian and dilatant fluids

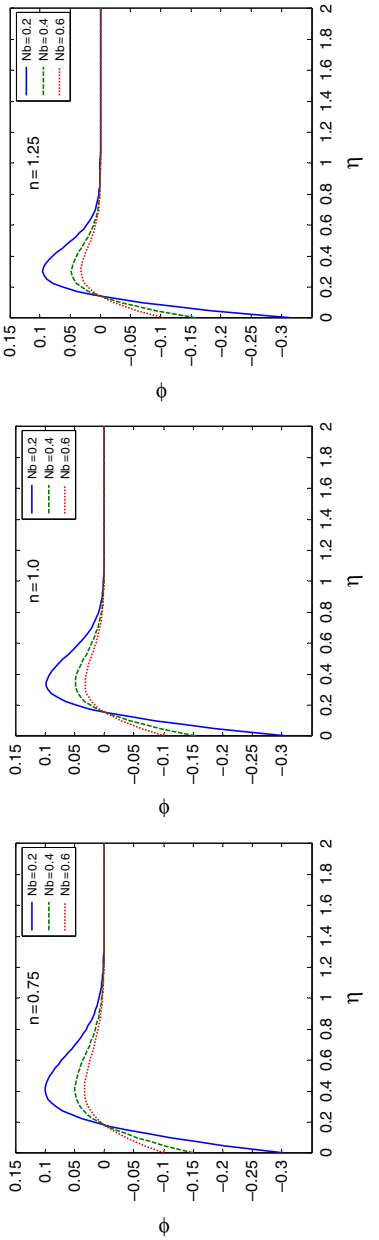

Figure 4.
Effect of Nb on nanoparticle volume fraction profiles for pseudo-plastic, Newtonian and dilatant fluids

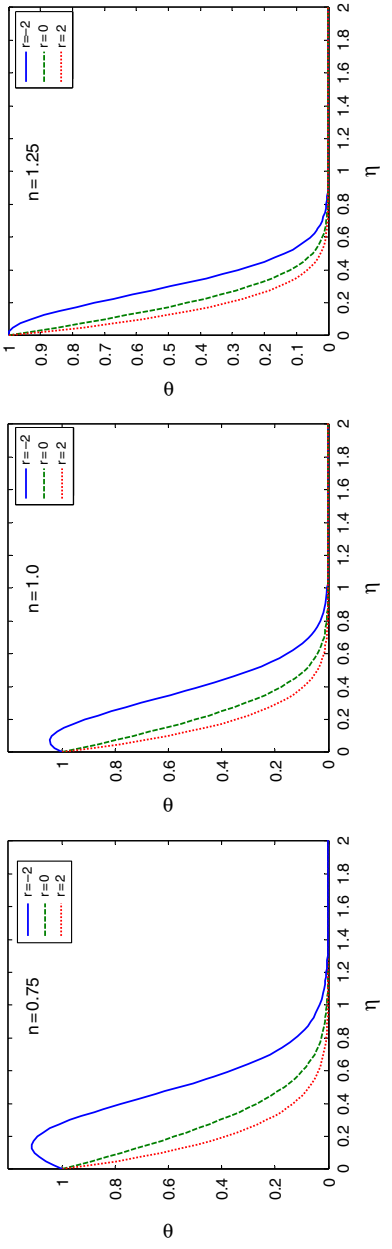

Figure 5.
Effect of r on temperature profiles for pseudo-plastic, Newtonian and dilatant fluids

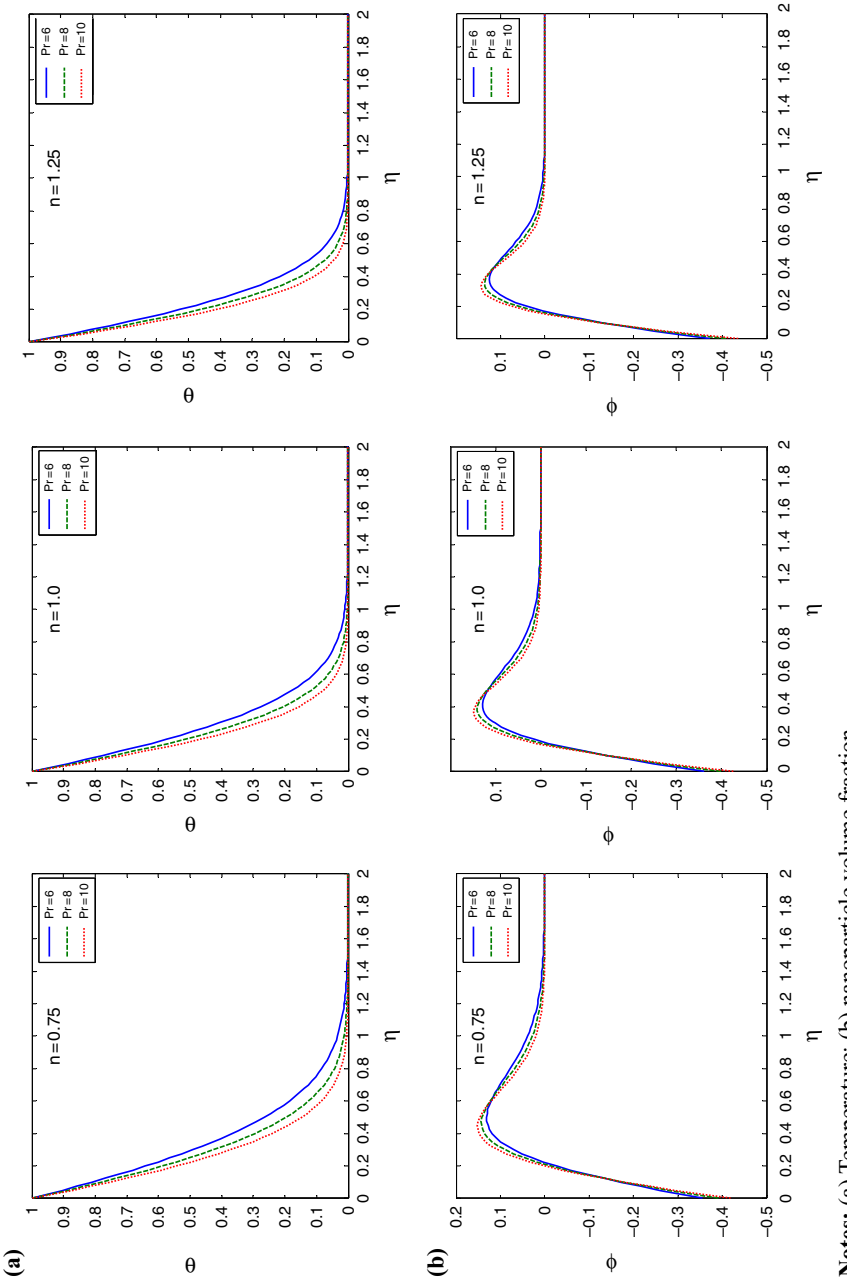

Figure 6.
Effect of *Pr* on temperature and nanoparticle volume fraction profiles for pseudo-plastic, Newtonian and dilatant fluids

Notes: (a) Temperature; (b) nanoparticle volume fraction

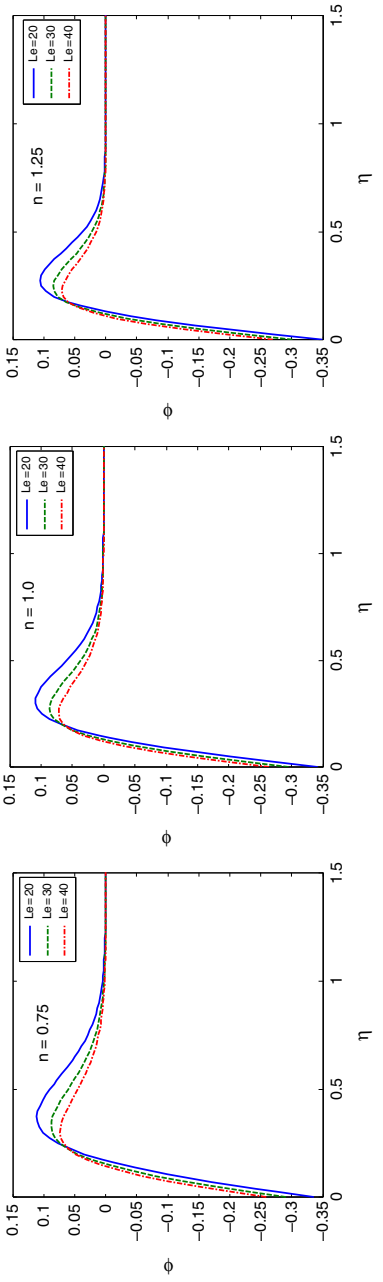

Figure 7.
Effect of Le on nanoparticle volume fraction profiles for pseudo-plastic, Newtonian and dilatant fluids

a lower Brownian motion coefficient D_B having a kinematic viscosity ν. Due to that, higher Lewis number reduces the nanoparticles volume fraction and its boundary layer thickness.

The numerical results for the Nusselt number and the Sherwood number values vs the thermopheresis parameter Nt and the Brownian motion Nb are presented in Figures 8 and 9. It is evident from Figure 8 that the value of the Nusselt number decreases with the increase of thermopheresis parameter Nt for both Newtonian and non-Newtonian fluids. It can also be seen that the Nusselt number decreases with the increase in the power-law fluid index n. The variation of the Sherwood number decreases as the thermophoresis parameter Nt increases. As the power-law fluid index n increases, the Sherwood number increases. It is clear from Figure 9 that the Nusselt number decreases with the increase in the power-law fluid index n. It is also noticed that there is no Brownian motion effect on the Nusselt number. It is evident from the figure that the effect of Brownian motion Nb is to increase the Sherwood number.

5. Conclusions

The problem of boundary layer flow and heat mass transfer of non-Newtonian power-law nanofluid over a non-linear stretching sheet is studied. The governing equations describing the problem are transformed into a nonlinear ordinary differential equations by suitable similarity transformations. The coupled nonlinear ordinary differential

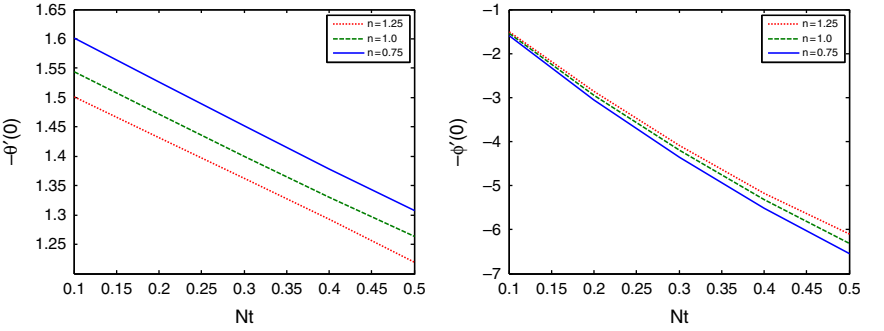

Figure 8.
Nusselt number and Sherwood number vs Nt

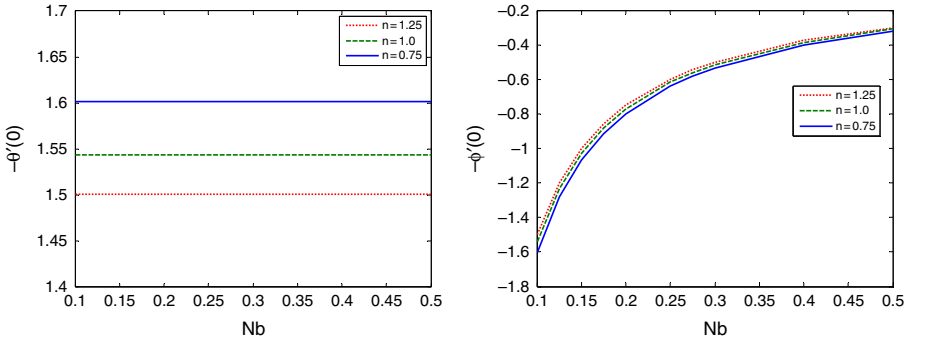

Figure 9.
Nusselt number and Sherwood number vs Nb

equations solved by using variational finite element method. It is found that with the increase of power-law index n is to increase the velocity profiles, and decreases the temperature and concentration profiles. The effect of velocity exponent parameter m is reduces the velocity profiles f". The temperature profiles are increases with the effect of thermophoresis parameter Nt and temperature exponent parameter r. It can be seen that the effect Brownian motion Nb, Prandtl number Pr and Lewis number Le reduces the nanoparticles volume fraction profiles on the other hand the effect of thermophoresis Nt increases nanoparticles volume fraction profiles. The Nusselt number coefficient $-\theta'(0)$ increases by increasing the Prandtl number Pr, stretching sheet parameter m and decreases by increasing the power-law index n, thermophoresis parameter Nt and Lewis number Le. Increases in the stretching sheet parameter m, Prandtl number Pr and thermophoresis parameter Nt decrease the Sherwood number coefficient $-\phi'(0)$ values. The effects of the Brownian motion parameter Nb and Lewis number Le lead to increases in the Sherwood number coefficient $-\phi'(0)$ values.

References

Acrivos, A. (1960), "A Theoretical analysis of laminar natural convection heat transfer to non-Newtonian fluids", *AIChE Journal*, Vol. 6 No. 4, pp. 584-590.

Acrivos, A., Shah, M.J. and Peterson, E.E. (1960), "Momentum and heat transfer in laminar boundary layer flows of non-Newtonian fluids past external surfaces", *AIChE Journal*, Vol. 6 No. 2, pp. 312-317.

Andersson, H.I. and Kumaran, V. (2006), "On sheet-driven motion of power-law fluids", *International Journal of Non-Linear Mechanics*, Vol. 41 No. 10, pp. 1228-1234.

Bachok, N., Ishak, A. and Pop, I. (2010), "Boundary layer flow of nanofluid over a moving surface in a flowing fluid", *International Journal of Thermal Sciences*, Vol. 49 No. 9, pp. 1663-1668.

Chamkha, A.J. and Al-Humoud, J. (2007), "Mixed convection heat and mass transfer of non-Newtonian fluids from a permeable surface embedded in a porous medium", *International Journal of Numerical Methods for Heat & Fluid Flow*, Vol. 17 No. 2, pp. 195-212.

Chamkha, A.J., Rashad, A.M. and Gorla, R. (2014), "Non-similar solutions for mixed convection along a wedge embedded in a porous medium saturated by a non-Newtonian nanofluid", *International Journal for Numerical Methods in Heat and Fluid Flow*, Vol. 24 No. 7, pp. 1471-1486.

Chen, C.H. (2008), "Effects of magnetic field and suction/injection on convection heat transfer of non-Newtonian power-law fluids past a power-law stretched sheet with surface heat flux", *International Journal of Thermal Sciences*, Vol. 47 No. 7, pp. 954-961.

Choi, S.U.S. (2009), "Nanofluids: from vision to reality through research", *Journal of Heat Transfer*, Vol. 131 No. 3, pp. 1-9.

Choi, S.U.S., Zhang, Z.G., Yu, W., Lockwood, F.E. and Grulke, E.A. (2001), "Anomalously thermal conductivity enhancement in nanotube suspensions", *Applied Physics Letters*, Vol. 79 No. 14, pp. 2252-2254.

Cortell, R. (2007), "Viscous flow and heat transfer over a non-linearly stretching sheet", *Applied Mathematics and Computation*, Vol. 184 No. 2, pp. 864-873.

Crane, L.J. (1970), "Flow past a stretching plate", *Zeitschrift für angewandte Mathematik und Physik*, Vol. 21 No. 4, pp. 645-647.

Denier, J.P. and Dabrowski, P.P. (2004), "On the boundary layer equations for power-law fluids", *Proceedings of the Royal Society of London*, Vol. 460 No. 2051, pp. 3143-3158.

Ellahi, R., Raza, M. and Vafai, K. (2012), "Series solutions of non-Newtonian nanofluids with Reynolds model and Vogelâs model by means of the homotopy analysis method", *Mathematical and Computer Modelling*, Vol. 55 Nos 7-8, pp. 1876-1891.

Fox, V.G., Erickson, L.E. and Fan, L.T. (1969), "The laminar boundary layer on a moving continuous flat sheet immersed in a non-Newtonian fluid", *AIChE Journal*, Vol. 15 No. 3, pp. 327-333.

Gorla, R.S.R. and Chamkha, A.J. (2011), "Natural convective boundary layer flow over a vertical plate embedded in a porous medium saturated with a non-Newtonian nanofluid", *International Journal of Microscale and Nanoscale Thermal and Fluid Transport Phenomena*, Vol. 3 No. 2, pp. 131-150.

Gorla, R.S.R. and Chamkha, A.J. (2013), "Free convection past a vertical plate embedded in a porous medium saturated with a non-Newtonian nanofluid", *Journal of Nanofluids*, Vol. 2 No. 4, pp. 297-302.

Hang, X. and Shi-Jun, L. (2009), "Laminar flow and heat transfer in the boundary-layer of non-Newtonian fluids over a stretching flat sheet", *Computers and Mathematics with Applications*, Vol. 57 No. 9, pp. 1425-1431.

Keimanesh, M., Rashidi, M.M., Chamkha Ali, J. and Jafari, R. (2011), "Study of a third grade non-Newtonian fluid flow between two parallel plates using the multi-step differential transform method", *Computers and Mathematics with Applications*, Vol. 62 No. 8, pp. 2871-2891.

Khan, W.A. and Pop, I. (2010), "Boundary-layer flow of a nanofluid past a stretching sheet", *International Journal of Heat Mass Transfer*, Vol. 53 Nos 11-12, pp. 2477-2483.

Khanafer, K., Vafai, K. and Lightstone, M. (2003), "Buoyancy-driven heat transfer enhancement in a two-dimensional enclosure utilizing nanofluids", *International Journal of Heat and Mass Transfer*, Vol. 46 No. 19, pp. 3639-3653.

Kishan, N. and Kavitha, P. (2014), "Magneto-hydro dynamic flow and heat transfer of non-Newtonian power-law fluid over a non-linear stretching surface with viscous dissipation", *International Journal of Applied Mechanics and Engineering*, Vol. 19 No. 2, pp. 259-273.

Kishan, N. and Shashidhar Reddy, B. (2013), "MHD effects on non-Newtonian power-law fluid past a continuously moving porous flat plate with heat flux and viscous dissipation", *International Journal of Applied Mechanics and Engineering*, Vol. 18 No. 2, pp. 425-445.

Kuznetsov, A.V. and Nield, D.A. (2010), "Natural convective boundary layer flow of a nanofluid past a vertical plate", *International Journal of Thermal Sciences*, Vol. 49 No. 2, pp. 243-247.

Kuznetsov, A.V. and Nield, D.A. (2014), "Natural convective boundary-layer flow of a nanofluid past a vertical plate: a revised model", *International Journal of Thermal Sciences*, Vol. 77, pp. 126-129.

Lotfi, R., Saboohi, Y. and Rashidi, A.M. (2010), "Numerical study of forced convective heat transfer of nanofluids: comparison of different approaches", *International Communications in Heat and Mass Transfer*, Vol. 37 No. 1, pp. 74-78.

Mahmoud, M.A.A. (2010), "Chemical reaction and variable viscosity effects on flow and mass transfer of a non-Newtonian visco-elastic fluid past a stretching surface embedded in a porous medium", *Meccanica*, Vol. 45 No. 6, pp. 835-846.

Makinde, O.D. and Aziz, A. (2011), "Boundary layer flow of a nanofluid past astretching sheet with a convective boundary condition", *International Journal of Thermal Sciences*, Vol. 50 No. 7, pp. 1326-1332.

Metzner, A.B. (1965), "Heat transfer in non-Newtonian fluid", *Advances in Heat Transfer*, Vol. 2, pp. 357-397.

Nield, D.A. (2011), "A note on the onset of convection in a layer of a porous medium saturated by a non-Newtonian nanofluids of power-law type", *Transport in Porous Media*, Vol. 87 No. 1, pp. 121-123.

Rashidi, M.M., Rastegari, M.T., Asadi, M. and Anwar Beg, O. (2012), "A study of non-Newtonian flow and heat transfer over a non-isothermal wedge using the homotopy analysis method", *Chemical Engineering Communications*, Vol. 199 No. 2, pp. 231-256.

Sakiadis, B.C. (1961), "Boundary layer behavior on continuous solid surfaces", *AIChE Journal*, Vol. 7 No. 1, pp. 26-28.

Schowalter, W.R. (1960), "The application of boundary layer theory to power-law pseudo plastic fluid similar solutions", *AIChE Journal*, Vol. 6, pp. 24-28.

Corresponding author
A. Chamkha can be contacted at: achamkha@yahoo.com